

A polynomial delay algorithm for the enumeration of bubbles with length constraints in directed graphs and its application to the detection of alternative splicing in RNA-seq data

Gustavo Sacomoto, Vincent Lacroix, and Marie-France Sagot

¹ INRIA Rhône-Alpes, 38330 Montbonnot Saint-Martin, France

² Université de Lyon, F-69000 Lyon; Université Lyon 1; CNRS, UMR5558, Laboratoire de Biométrie et Biologie Évolutive, F-69622 Villeurbanne, France
{gustavo.sacomoto, Marie-France.Sagot}@inria.fr,
vincent.lacroix@univ-lyon1.fr

Abstract. We present a new algorithm for enumerating bubbles with length constraints in directed graphs. This problem arises in transcriptomics, where the question is to identify all alternative splicing events present in a sample of mRNAs sequenced by RNA-seq. This is the first polynomial-delay algorithm for this problem and we show that in practice, it is faster than previous approaches. This enables us to deal with larger instances and therefore to discover novel alternative splicing events, especially long ones, that were previously overseen using existing methods.

1 Introduction

Transcriptomes of model or non model species can now be studied by sequencing, through the use of RNA-seq, a protocol which enables us to obtain, from a sample of RNA transcripts, a (large) collection of (short) sequencing reads, using Next Generation Sequencing (NGS) technologies [15,10]. Nowadays, a typical experiment produces 100M reads of 100nt each. However, the original RNA molecules are longer (typically 500-3000nt) and the general computational problem in the area is then to be able to assemble the reads in order to reconstruct the original set of transcripts. This problem is not trivial for mainly two reasons. First, genomes contain repeats that may be longer than the read length. Hence, a read does not necessarily enable to identify unambiguously the locus from which the transcript was produced. Second, each genomic locus may generate several types of transcripts, either because of genomic variants (i.e. there may exist several alleles for a locus) or because of transcriptomic variants (i.e. alternative splicing or alternative transcription start/end may generate several transcripts from a single locus that differ by the inclusion or exclusion of subsequences). Hence, if a read matches a subsequence shared by several alternative transcripts, it is a priori not possible to decide which of these transcripts generated the read.

General purpose transcriptome assemblers [7,12,14] aim at the general goal of identifying all alternative transcripts, but because of the extensive use of heuristics, they usually fail to identify infrequent transcripts, tend to report several fragments for each gene, or fuse genes that share repeats. Local transcriptome assemblers [13], on the other hand, aim at a simpler goal, as they do not reconstruct full length transcripts. Instead, they focus on reporting all variable regions (polymorphisms): whether genomic (SNPs, indels) or transcriptomic (alternative splicing events). They are much less affected by the issue of repeats, since they focus only on the variable regions. They can afford to be exact and therefore are able to have access to infrequent transcripts. The fundamental idea is that each polymorphism corresponds to a recognizable pattern, called a bubble in the de Bruijn graph built from the RNA-seq reads. In practice, only bubbles with specific length constraints are of interest. However, even with this restriction, the number of such bubbles can be exponential in the size of the graph. Therefore, as with other enumeration problems, the best possible algorithm is one spending time polynomial in the input size between the output of two bubbles, i.e. a polynomial delay algorithm

In this paper, we introduce the first polynomial delay algorithm to enumerate all bubbles with length constraints in a weighted directed graph. Its complexity in the best theoretical case for general graphs is $O(n(m+n \log n))$ (Section 3) where n is the number of vertices in the graph, m the number of arcs. In the particular case of de Bruijn graphs, the complexity is $O(n(m+n \log \alpha))$ (Section 4.1) where α is a constant related to the length of the skipped part in an alternative splicing event. In practice, an algorithmic solution in $O(nm \log n)$ (Section 4.2) appears to work better on de Bruijn graphs built from such data. We implemented the latter, show that it is more efficient than previous approaches and outline that it enables us to discover novel long alternative splicing events.

2 De Bruijn graphs and alternative splicing

A *de Bruijn graph* (DBG) is a directed graph $G = (V, A)$ whose vertices V are labeled by words of length k over an alphabet Σ . An arc in A links a vertex u to a vertex v if the suffix of length $k-1$ of u is equal to the prefix of v . The out and the in-degree of any vertex are therefore bounded by the size of the alphabet Σ . In the case of NGS data, the k -mers correspond to all words of length k present in the reads of the input dataset, and only those. In relation to the classical de Bruijn graph for all possible words of size k , the DBG for NGS data may then not be complete. Given two vertices s and t in G , an (s, t) -path is a path from s to t . As defined in [3], by an (s, t) -bubble, we mean two vertex-disjoint (s, t) -paths. This definition is, of course, not restricted to de Bruijn graphs.

As was shown in [13], polymorphisms (i.e. variable parts) in a transcriptome (including alternative splicing (AS) events) correspond to recognizable patterns in the DBG that are precisely the (s, t) -bubbles. Intuitively, the variable parts correspond to alternative paths and the common parts correspond to the beginning and end points of those paths. More formally, any process generating

patterns awb and $aw'b$ in the sequences, with $a, b, w, w' \in \Sigma^*$, $|a| \geq k, |b| \geq k$ and w and w' not sharing any k -mer, creates a (s, t) -bubble in the DBG. In the special case of AS events excluding mutually exclusive exons, since w' is empty, one of the paths corresponds to the *junction* of ab , i.e. to k -mers that contain at least one letter of each sequence. Thus the number of vertices of this path in the DBG is predictable: it is at most³ $k - 1$. An example is given in Fig. 2. In practice [13], an upper bound α to the other path and a lower bound β on both paths is also imposed. In other words, an AS event corresponds to a (s, t) -bubble with paths p_1 and p_2 such that p_1 has at most α vertices, p_2 at most $k - 1$ and both have at least β vertices.

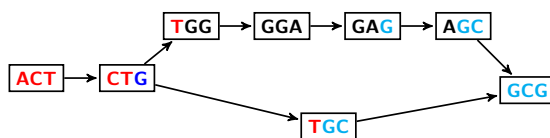


Fig. 1. DBG with $k = 3$ for the sequences: $ACTGGAGCG$ (awb) and $ACTGCG$ (ab). The pattern in the sequence generates a (s, t) -bubble, from CTG to GCG . In this case, $b = GCG$ and $w = GGA$ have their first letter G in common, so the path corresponding to the junction ab has $k - 1 - 1 = 1$ vertex.

Given a directed graph G with *non-negative* arc weights $w : E \mapsto \mathbb{Q}_{\geq 0}$, the length of the path $p = (v_0, v_1) \dots (v_{n-1}, v_n)$ is the sum of the weights of the edges in p and is denoted by $|p|$. The distance, length of the shortest path, from u to v is denoted by $d(u, v)$. We extend the definition of bubble given above.

Definition 1 ($(s, t, \alpha_1, \alpha_2)$ -bubble). A $(s, t, \alpha_1, \alpha_2)$ -bubble in a weighted directed graph is a (s, t) -bubble with paths p_1, p_2 satisfying $|p_1| \leq \alpha_1$ and $|p_2| \leq \alpha_2$.

In practice, when dealing with DBGs built from NGS data, in a lossless preprocessing step, all maximal non-branching linear paths of the graph (i.e. paths containing only vertices with in and out-degree 1) are compressed each into one single vertex, whose label corresponds to the label of the path (i.e. it is the concatenation of the labels of the vertices in the path without the overlapping part(s)). The resulting graph is the *compressed de Bruijn graph* (cDBG). In the cDBG, the vertices can have labels larger than k , but an arc still indicates a suffix-prefix overlap of size $k - 1$. Finally, since the only property of a bubble corresponding to an AS event is the constraint on the length of the path, we can disregard the labels from the cDBG and only keep for each vertex its label length⁴. In this way, searching for bubbles corresponding to AS events in a cDBG

³ The size is *exactly* $k - 1$ if w has no common prefix with b and no common suffix with a .

⁴ Resulting in a graph with weights in the vertices. Here, however, we consider the weights in the arcs. Since this is more standard and, in our case, both alternatives are equivalent, we can transform one into another by splitting vertices or arcs.

can be seen as a particular case of looking for $(s, t, \alpha_1, \alpha_2)$ -bubbles satisfying the lower bound β in a non-negative weighted directed graph.

Actually, it is not hard to see that the enumeration of $(s, t, \alpha_1, \alpha_2)$ -bubbles, for all s and t , satisfying the lower bound β is NP-hard. Indeed, deciding the existence of at least one $(s, t, \alpha_1, \alpha_2)$ -bubble, for some s and t , with the lower bound β in a weighted directed graph where all the weights are 1 is NP-complete. It follows by a simple reduction from the Hamiltonian st -path problem [6]: given a directed graph $G = (V, E)$ and two vertices s and t , build the graph G' by adding to G the vertices s' and t' , the arcs (s, s') and (t, t') , and a new path from s' to t' with exactly $|V|$ nodes. There is a $(x, y, |V| + 2, |V| + 2)$ -bubble, for some x and y , satisfying the lower bound $\beta = |V| + 2$ in G' if and only if there is a Hamiltonian path from s to t in G .

From now on, we consider the enumeration of all $(s, t, \alpha_1, \alpha_2)$ -bubbles (without the lower bound) for a given source (fixed s) in a non-negative weighted directed graph G (not restricted to a cDBG). The number of vertices and arcs of G is denoted by n and m , respectively.

3 An $O(n(m + n \log n))$ delay algorithm

In this section, we present an $O(n(m + n \log n))$ delay algorithm to enumerate, for a fixed source s , all $(s, t, \alpha_1, \alpha_2)$ -bubbles in a general directed graph G with non-negative weights. In a *polynomial delay* enumeration algorithm, the time elapsed between the output of two solutions is polynomial in the instance size. The pseudocode is shown in Algorithm 1. It is important to stress that this pseudocode uses high-level primitives, e.g. the tests in lines 5, 11 and 19. An efficient implementation for the test in line 11, along with its correctness and analysis, is implicitly given in Lemma 3. This is a central result in this section. For its proof we need Lemma 1.

Algorithm 1 uses a recursive strategy, inspired by the binary partition method, that successively divides the solution space at every call until the considered subspace is a singleton. In order to have a more symmetric structure for the subproblems, we define the notion of a *pair of compatible paths*, which is an object that generalizes the definition of a $(s, t, \alpha_1, \alpha_2)$ -bubble. Given two vertices $s_1, s_2 \in V$ and upper bounds $\alpha_1, \alpha_2 \in \mathbb{Q}_{\geq 0}$, the paths $p_1 = s_1 \rightsquigarrow t_1$ and $p_2 = s_2 \rightsquigarrow t_2$ are a *pair of compatible paths* for s_1 and s_2 if $t_1 = t_2$, $|p_1| \leq \alpha_1$, $|p_2| \leq \alpha_2$ and the paths are internally vertex-disjoint. Clearly, every $(s, t, \alpha_1, \alpha_2)$ -bubble is also a pair of compatible paths for $s_1 = s_2 = s$ and some t .

Given a vertex v , the set of out-neighbors of v is denoted by $\delta^+(v)$. Let now $\mathcal{P}_{\alpha_1, \alpha_2}(s_1, s_2, G)$ be the set of all pairs of compatible paths for s_1, s_2, α_1 and α_2 in G . We have⁵ that:

$$\mathcal{P}_{\alpha_1, \alpha_2}(s_1, s_2, G) = \mathcal{P}_{\alpha_1, \alpha_2}(s_1, s_2, G') \bigcup_{v \in \delta^+(s_2)} (s_2, v) \mathcal{P}_{\alpha_1, \alpha_2'}(s_1, v, G - s_2), \quad (1)$$

⁵ The same relation is true using s_1 instead of s_2 .

where $\alpha'_2 = \alpha_2 - w(s_2, v)$ and $G' = G - \{(s_2, v) | v \in \delta^+(s_2)\}$. In other words, the set of pairs of compatible paths for s_1 and s_2 can be partitioned into: $\mathcal{P}_{\alpha_1, \alpha'_2}(s_1, v, G - s_2)$, the sets of pairs of paths containing the arc (s_2, v) , for each $v \in \delta^+(s_2)$; and $\mathcal{P}_{\alpha_1, \alpha_2}(s_1, s_2, G')$, the set of pairs of paths that do not contain any of them. Algorithm 1 implements this recursive partition strategy. The solutions are only output in the leaves of the recursion tree (line 3), where the partition is always a singleton. Moreover, in order to guarantee that every leaf in the recursion tree outputs at least one solution, we have to test if $\mathcal{P}_{\alpha_1, \alpha'_2}(s_1, v, G - s_2)$ (and $\mathcal{P}_{\alpha_1, \alpha_2}(s_1, s_2, G')$) is not empty before making the recursive call (lines 11 and 19).

Algorithm 1: `enumerate_bubbles`($s_1, \alpha_1, s_2, \alpha_2, B, G$)

```

1 if  $s_1 = s_2$  then
2   if  $B \neq \emptyset$  then
3     output( $B$ )
4     return
5   else if there is no  $(s, t, \alpha_1, \alpha_2)$ -bubble, where  $s = s_1 = s_2$  then
6     return
7   end
8 end
9 choose  $u \in \{s_1, s_2\}$ , such that  $\delta^+(u) \neq \emptyset$ 
10 for  $v \in \delta^+(u)$  do
11   if there is a pair of compatible paths using  $(u, v)$  in  $G$  then
12     if  $u = s_1$  then
13       enumerate_bubbles( $v, \alpha_1 - w(s_1, v), s_2, \alpha_2, B \cup (s_1, v), G - s_1$ )
14     else
15       enumerate_bubbles( $s_1, \alpha_1, v, \alpha_2 - w(s_2, v), B \cup (s_2, v), G - s_2$ )
16     end
17   end
18 end
19 if there is a pair of compatible paths in  $G - \{(u, v) | v \in \delta^+(u)\}$  then
20   enumerate_bubbles( $v, \alpha_1, s_2, \alpha_2, B, G - \{(u, v) | v \in \delta^+(u)\}$ )
21 end

```

The correctness of Algorithm 1 follows directly from the relation given in Eq. 1 and the correctness of the tests performed in lines 11 and 19. In the remaining of this section, we describe a possible implementation for the tests, prove correctness and analyze the time complexity. Finally, we prove that Algorithm 1 has an $O(n(m + n \log n))$ delay.

Lemma 1. *There exists a pair of compatible paths for $s_1 \neq s_2$ in G if and only if there exists t such that $d(s_1, t) \leq \alpha_1$ and $d(s_2, t) \leq \alpha_2$.*

Proof. Clearly this is a necessary condition. Let us prove that it is also sufficient. Consider the paths $p_1 = s_1 \rightsquigarrow t$ and $p_2 = s_2 \rightsquigarrow t$, such that $|p_1| \leq \alpha_1$ and

$|p_2| \leq \alpha_2$. Let t' be the first vertex in common between p_1 and p_2 . The sub-paths $p'_1 = s_1 \rightsquigarrow t'$ and $p'_2 = s_2 \rightsquigarrow t'$ are internally vertex-disjoint, and since the weights are non-negative, they also satisfy $|p'_1| \leq |p_1| \leq \alpha_1$ and $|p'_2| \leq |p_2| \leq \alpha_2$.

Using this lemma, we can test for the existence of a pair of compatible paths for $s_1 \neq s_2$ in $O(m + n \log n)$ time. Indeed, let T_1 be a shortest path tree of G rooted in s_1 and truncated at distance α_1 , the same for T_2 , meaning that, for any vertex w in T_1 (resp. T_2), the tree path between s_1 and w (resp. s_2 and w) is a shortest one. It is not difficult to prove that the intersection $T_1 \cap T_2$ is not empty if and only if there is a pair of compatible paths for s_1 and s_2 in G . Moreover, each shortest path tree can be computed in $O(m + n \log n)$ time, using Dijkstra's algorithm [6]. Thus, in order to test for the existence of a $(s, t, \alpha_1, \alpha_2)$ -bubble for some t in G , we can test, for each arc (s, v) outgoing from s , the existence of a pair of compatible paths for $s \neq v$ and v in G . Since s has at most n out-neighbors, we obtain Lemma 2.

Lemma 2. *The test of line 5 can be performed in $O(n(m + n \log n))$.*

The test of line 11 could be implemented using the same idea. For each $v \in \delta^+(u)$, we test for the existence of a pair of compatible paths for, say, $u = s_2$ (the same would apply for s_1) and v in $G - u$, that is v is in the subgraph of G obtained by eliminating from G the vertex u and all the arcs incoming to or outgoing from u . This would lead to a total cost of $O(n(m + n \log n))$ for all tests of line 11 in each call. However, this is not enough to achieve an $O(n(m + n \log n))$ delay. In Lemma 3, we present an improved strategy to perform these tests in $O(m + n \log n)$ total time.

Lemma 3. *The test of line 11, for all $v \in \delta^+(u)$, can be performed in $O(m + n \log n)$ total time.*

Proof. Let us assume that $u = s_2$, the case $u = s_1$ is symmetric. From Lemma 1, for each $v \in \delta^+(u)$, we have that deciding if there exists a pair of compatible paths for s_1 and s_2 in G that uses (u, v) is equivalent to deciding if there exists t satisfying (i) $d(s_1, t) \leq \alpha_1$ and (ii) $d(v, t) \leq \alpha_2 - w(u, v)$ in $G - u$.

First, we compute a shortest path tree rooted in s_1 for $G - u$. Let V_{α_1} be the set of vertices at a distance at most α_1 from s_1 . We build a graph G' by adding a new vertex r to $G - u$, and for each $y \in V_{\alpha_1}$, we add the arcs (y, r) with weight $w(y, r) = 0$. We claim that there exists t in $G - u$ satisfying conditions (i) and (ii) if and only if $d(v, r) \leq \alpha_2 - w(u, v)$ in G' . Indeed, if t satisfies (i) we have that the arc (t, r) is in G' , so $d(t, r) = 0$. From the triangle inequality and (ii), $d(v, r) \leq d(v, t) + d(t, r) = d(v, t) \leq \alpha_2 - w(u, v)$. The other direction is trivial.

Finally, we compute a shortest path tree T_r rooted in r for the reverse graph G'^R , obtained by reversing the direction of the arcs of G' . With T_r , we have the distance from any vertex to r in G' , i.e. we can answer the query $d(v, r) \leq \alpha_2 - w(u, v)$ in constant time. Observe that the construction of T_r depends only on $G - u$, s_1 and α_1 , i.e. T_r is the same for all out-neighbors $v \in \delta^+(u)$. Therefore, we can build T_r only once in $O(m + n \log n)$ time, with two iterations of Dijkstra's algorithm, and use it to answer each test of line 11 in constant time.

Theorem 1. *Algorithm 1 has $O(n(m + n \log n))$ delay.*

Proof. The height of the recursion tree is bounded by $2n$ since at each call the size of the graph is reduced either by one vertex (lines 13 and 15) or all its out-neighborhood (line 20). After at most $2n$ recursive calls, the graph is empty. Since every leaf of the recursion tree outputs a solution and the distance between two leaves is bounded by $4n$, the delay is $O(n)$ multiplied by the cost per node (call) in the recursion tree. From Lemma 1, line 19 takes $O(m + n \log n)$ time, and from Lemma 3, line 11 takes $O(m + n \log n)$ total time. This leads to an $O(m + n \log n)$ time per call, excluding line 5. Lemma 2 states that the cost for the test in line 5 is $O(n(m + n \log n))$, but this line is executed only once, at the root of the recursion tree. Therefore, the delay is $O(n(m + n \log n))$.

4 Implementation and experimental results

We now discuss the details necessary for an efficient implementation of Algorithm 1 and the results on two sets of experimental tests. For the first set, our goal is to compare the running time of Dijkstra’s algorithm (for typical DBGs arising from applications) using several priority queue implementations. With the second set, our objective is to compare an implementation of Algorithm 1 to the KISSPLICE algorithm [13]. For both cases, we retrieved from the *Short Read Archive* (accession code ERX141791) 14M Illumina 79bp single-ended reads of a *Drosophila melanogaster* RNA-seq experiment. We then built the de Bruijn graph for this dataset with $k = 31$ using the MINIA algorithm [5]. In order to remove likely sequencing errors, we discarded all k -mers that are present less than 3 times in the dataset. The resulting graph contained 22M k -mers, which after compressing all maximal linear paths, corresponded to 600k vertices.

In order to perform a fair comparison with KISSPLICE, we pre-processed the graph as described in [13]. Namely, we decomposed the underlying undirected graph into biconnected components (BCCs) and compressed all non-branching bubbles with equal path lengths. In the end, after discarding all BCCs with less than 4 vertices (as they cannot contain a bubble), we obtained 7113 BCCs, the largest one containing 24977 vertices. This pre-processing is lossless, i.e. every bubble in the original graph is entirely contained in exactly one BCC. In KISSPLICE, the enumeration is then done in each BCC independently.

4.1 Dijkstra’s algorithm with different priority queues

Dijkstra’s algorithm is an important subroutine of Algorithm 1 that may have a big influence on its running time. Actually, the time complexity of Algorithm 1 can be written as $O(nc(n, m))$, where $c(n, m)$ is the complexity of Dijkstra’s algorithm. There are several variants of this algorithm [6], with different complexities depending on the priority queue used, including binary heaps ($O(m \log n)$) and Fibonacci heaps ($O(m + n \log n)$). In the particular case where all the weights are non-negative integers bounded by C , Dijkstra’s algorithm can be implemented

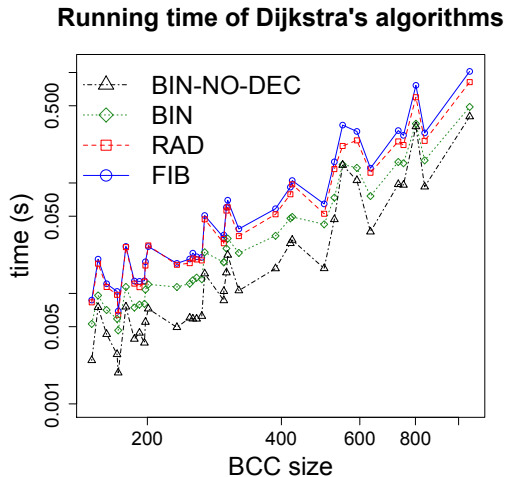


Fig. 2. Running times for each version of Dijkstra’s algorithm: using Fibonacci heaps (FIB), using radix heaps (RAD), using binary heaps (BIN) and using binary heaps without the decrease-key operation (BIN-NO-DEC). The tests were done including all BCCs with more than 150 vertices. Both axes are in logarithmic scale.

using radix heaps ($O(m + n \log C)$) [2]. As stated in Section 2, the weights of the de Bruijn graphs considered here are integer, but not necessarily bounded. However, we can remove from the graph all arcs with weights greater than α_1 since these are not part of any $(s, t, \alpha_1, \alpha_2)$ -bubble. This results in a complexity of $O(m + n \log \alpha_1)$ for Dijkstra’s algorithm.

We implemented four versions of Lemma 2 (for deciding whether there exists a $(s, t, \alpha_1, \alpha_2)$ -bubble for a given s) each using a different version of Dijkstra’s algorithm: with Fibonacci heaps (FIB), with radix heaps (RAD), with binary heaps (BIN) and with binary heaps without decrease-key operation (BIN-NO-DEC). The last version is Dijkstra’s modified in order not to use the decrease-key operation so that we can use a simpler binary heap that does not support such operation [4]. We then ran the four versions, using $\alpha_1 = 1000$ and $\alpha_2 = 2k - 2 = 60$, for each vertex in all the BCCs with more than 150 vertices. The results are shown⁶ in Fig. 2. Contrary to the theoretical predictions, the versions with the best complexities, FIB and RAD, have the worst results on this type of instances. It is clear that the best version is BIN-NO-DEC, which is at least 2.2 times and at most 4.3 times faster than FIB. One of the factors possibly contributing to a better performance of BIN and BIN-NO-DEC is the fact that cDBGs, as stated in Section 2, have bounded degree and are therefore sparse.

⁶ The results for the largest BCC were omitted from the plot to improve the visualization. It took 942.15s for FIB and 419.84s for BIN-NO-DEC.

4.2 Comparison with the KISSPLICE algorithm

In this section, we compare Algorithm 1 to the KISSPLICE (version 1.8.1) enumeration algorithm [13]. To this purpose, we implemented Algorithm 1 using Dijkstra’s algorithm with binary heaps without the decrease-key operation for all shortest paths computation. In this way, the delay of Algorithm 1 becomes $O(nm \log n)$, which is worse than the one using Fibonacci or radix heaps, but is faster in practice. The goal of the KISSPLICE enumeration is to find all the potential alternative splicing events in a BCC, i.e. to find all $(s, t, \alpha_1, \alpha_2)$ -bubbles satisfying also the lower bound constraint (Section 2). In order to compare KISSPLICE to Algorithm 1, we (naively) modified the latter so that, whenever a $(s, t, \alpha_1, \alpha_2)$ -bubble is found, we check whether it also satisfies the lower bound constraints and output it only if it does.

In KISSPLICE, the upper bound α_1 is an open parameter, $\alpha_2 = k - 1$ and the lower bound is $k - 7$. Moreover, there are two stop conditions: either when more than 10000 $(s, t, \alpha_1, \alpha_2)$ -bubbles satisfying the lower bound constraint have been enumerated or a 900s timeout has been reached. We ran both KISSPLICE (version 1.8.1) and the modified Algorithm 1, with the stop conditions, for all 7113 BCCs, using $\alpha_2 = 60$, a lower bound of 54 and $\alpha_1 = 250, 500, 750$ and 1000. The running times for all BCCs with more than 150 vertices (there are 37) is shown⁷ in Fig. 3. For the BCCs smaller than 150 vertices, both algorithms have comparable (very small) running times. For instance, with $\alpha_1 = 250$, KISSPLICE runs in 17.44s for *all* 7113 BCCs with less than 150 vertices, while Algorithm 1 runs in 15.26s.

The plots in Fig. 3 show a trend of increasing running times for larger BCCs, but the graphs are not very smooth, i.e. there are some sudden decreases and increases in the running times observed. This is in part due to the fact that the time complexity of Algorithm 1 is output sensitive. The delay of the algorithm is $O(nm \log n)$, but the total time complexity is $O(|\mathcal{B}|nm \log n)$, where $|\mathcal{B}|$ is the number of $(s, t, \alpha_1, \alpha_2)$ -bubbles in the graph. The number of bubbles in the graph depends on its internal structure. A large graph does not necessarily have a large number of bubbles, while a small graph may have an exponential number of bubbles. Therefore, the value of $|\mathcal{B}|nm \log n$ can decrease by increasing the size of the graph.

Concerning now the comparison between the algorithms, as we can see in Fig. 3, Algorithm 1 is usually several times faster (keep in mind that the axes are in logarithmic scale) than KISSPLICE, with larger differences when α_1 increases (10 to 1000 times faster when $\alpha_1 = 1000$). In some instances however, KISSPLICE is faster than Algorithm 1, but (with only one exception for $\alpha_1 = 250$ and $\alpha_1 = 500$) they correspond either to very small instances or to cases where only 10000 bubbles were enumerated and the stop condition was met. Finally, using Algorithm 1, the computation finished within 900s for all but 3 BCCs, whereas using KISSPLICE, 11 BCCs remained unfinished after 900s. The improvement in

⁷ The BCCs where *both* algorithms reach the timeout were omitted from the plots to improve the visualization. For $\alpha_1 = 250, 500, 750$ and 1000 there are 1, 2, 3 and 3 BCCs omitted, respectively.

time therefore enables us to have access to bubbles that could not be enumerated with the previous approach.

4.3 On the usefulness of larger values of α_1

In the implementation of KISSPLICE [1], the value of α_1 was experimentally set to 1000 due to performance issues, as indeed the algorithm quickly becomes impractical for larger values. On the other hand, the results of Section 4.2 suggest that Algorithm 1, that is faster than KISSPLICE, can deal with larger values of α_1 . From a biological point of view, it is a priori possible to argue that $\alpha_1 = 1000$ is a reasonable choice, because 87% of annotated exons in *Drosophila* indeed are shorter than 1000nt [11]. However, missing the top 13% may have a big impact on downstream analyses of AS, not to mention the possibility that not yet annotated AS events could be enriched in long skipped exons. In this section, we outline that larger values of α_1 indeed produces more results that are biologically relevant. For this, we exploit another RNA-seq dataset, with deeper coverage.

To this purpose, we retrieved 32M RNA-seq reads from the human brain and 39M from the human liver from the Short Read Archive (accession number ERP000546). Next, we built the de Bruijn graph with $k = 31$ for both datasets, then merged and decomposed the DBG into 5692 BCCs (containing more than 10 vertices). We ran Algorithm 1 for each BCC with $\alpha_1 = 5000$. It took 4min25s for Algorithm 1 to run on all BCCs, whereas KISSPLICE, even using $\alpha_1 = 1000$, took 31min45s, almost 8 times more. There were 59 BCCs containing at least one bubble with the length of the longest path strictly larger than 1000bp potentially corresponding to alternative splicing events. In Fig. 4.3, we show one of those bubbles mapped to the reference genome. It corresponds to an exon skipping in the PRRC2B human gene, the skipped exon containing 2069 bp. While the transcript containing the exon is annotated, the variant with the exon skipped is not annotated.

Furthermore, we ran TRINITY [7] (the most widely used transcriptome assembler) on the same dataset and found that it was unable to report this novel variant. Our method therefore enables us to find new AS events, reported by no other method. This is, of course, just an indication of the usefulness of our approach when compared to a full-transcriptome assembler. A more systematic comparison with TRINITY, as done in [13], is out of the scope of this work.

5 A natural generalization

For the sake of theoretical completeness, in this section, we extend the definition of $(s, t, \alpha_1, \alpha_2)$ -bubble to the case where the length constraints concern d vertex-disjoint paths, for an arbitrary but fixed d .

Definition 2 ((s, t, A) - d -bubble). *Let d be a natural number and $A = \{\alpha_1, \dots, \alpha_d\} \subset \mathbb{Q}_{\geq 0}$. Given a directed weighted graph G and two vertices s and t , an (s, t, A) - d -bubble is a set of d pairwise internally vertex-disjoint paths $\{p_1, \dots, p_d\}$, satisfying $p_i = s \rightsquigarrow t$ and $|p_i| \leq \alpha_i$, for all $i \in [1, d]$.*

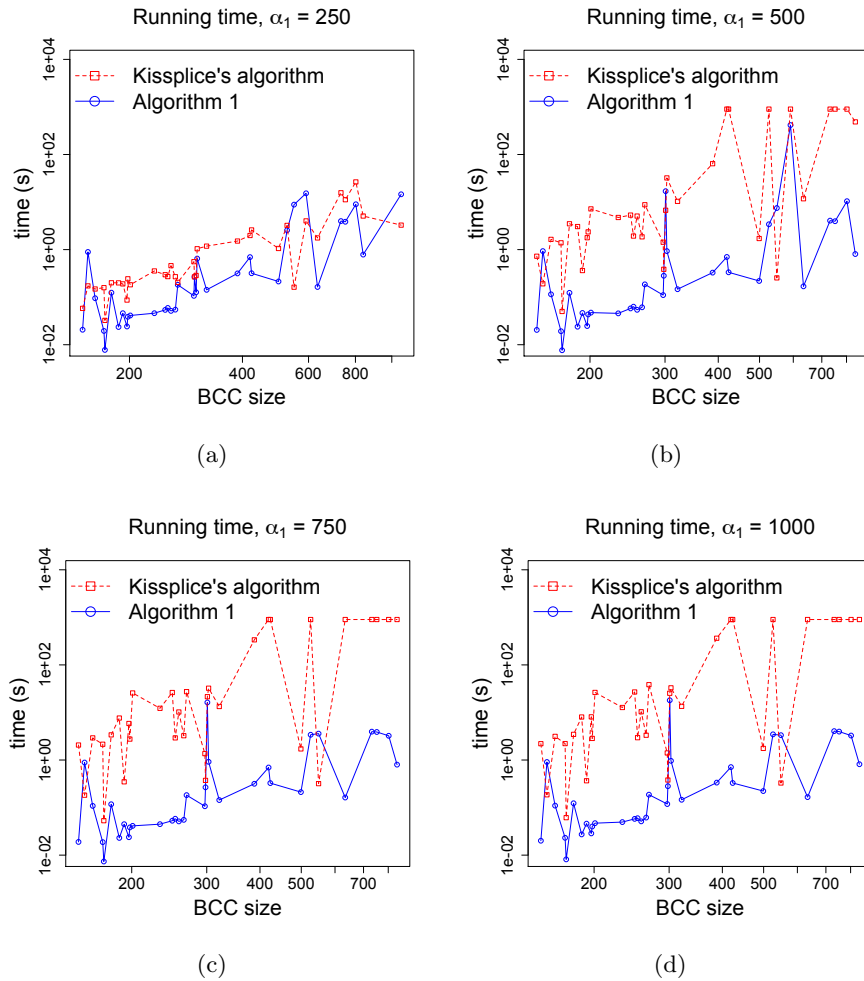


Fig. 3. Running times of Algorithm 1 and of the KISSPLICE algorithm [13] for all the BCCs with more than 150 vertices. Each graph (a), (b), (c) and (d) shows the running time of both algorithms for $\alpha_1 = 250, 500, 750$ and 1000 , respectively.

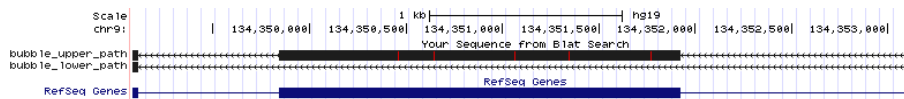


Fig. 4. One of the bubbles with longest path larger than 1000 bp found by Algorithm 1 with the corresponding sequences mapped to the reference genome and visualized using the UCSC Genome Browser. The first two lines correspond to the sequences of, respectively, the shortest (exon exclusion variant) and longest paths of the bubble mapped to the genome. The blue lines are the UCSC human transcript annotations.

Analogously to $(s, t, \alpha_1, \alpha_2)$ -bubbles, we can define two variants of the enumeration problem: all bubbles with a given source (s fixed) and all bubbles with a given source and target (s and t fixed). In both cases, the first step is to decide the existence of at least one (s, t, A) - d -bubble in the graph.

Problem 1 ((s, t, A)- d -bubble decision problem). Given a non-negatively weighted directed graph G , two vertices s, t , a set $A = \{\alpha_1, \dots, \alpha_d\} \subset \mathbb{Q}_{\geq 0}$ and $d \in \mathbb{N}$, decide if there exists a (s, t, A) - d -bubble.

This problem is a generalization of the two-disjoint-paths problem with a min-max objective function, which is NP-complete [9]. More formally, this problem can be stated as follows: given a directed graph G with non-negative weights, two vertices $s, t \in V$, and a maximum length M , decide if there exists a pair of vertex-disjoint paths such that the maximum of their lengths is less than M . The (s, t, A) - d -bubble decision problem, with $A = \{M, M\}$ and $d = 2$, is precisely this problem.

*Problem 2 (($s, *, A$)- d -bubble decision problem).* Given a non-negatively weighted directed graph G , a vertex s , a set $A = \{\alpha_1, \dots, \alpha_d\} \subset \mathbb{Q}_{\geq 0}$ and $d \in \mathbb{N}$, decide if there exists a (s, t, A) - d -bubble, for some $t \in V$.

The two-disjoint-path problem with a min-max objective function is NP-complete even for strictly positive weighted graphs. Let us reduce Problem 2 to it. Consider a graph G with strictly positive weights, two vertices $s, t \in V$, and a maximum length M . Construct the graph G' by adding an arc with weights 0 from s to t and use this as input for the $(s, *, \{M, M, 0\})$ -3-bubble decision problem. Since G has strictly positive weights, the only path with length 0 from s to t in G' is the added arc. Thus, there is a $(s, *, \{M, M, 0\})$ -3-bubble in G' if and only if there are two vertex-disjoint paths in G each with a length $\leq M$.

Therefore, the decision problem for fixed s (Problem 1) is NP-hard for $d \geq 2$, and for fixed s and t (Problem 2) is NP-hard for $d \geq 3$. In other words, the only tractable case is the enumeration of (s, t, A) -2-bubbles with fixed s , the one considered in Section 3.

6 Conclusion

We introduced a polynomial delay algorithm which enumerates all bubbles with length constraints in directed graphs. We show that it is faster than previous approaches and therefore enables us to enumerate more bubbles. These additional bubbles correspond to longer AS events, overseen previously, but biologically very relevant. As shown in [2], by combining radix and Fibonacci heaps in Dijkstra, we can achieve a complexity in $O(n(m + n\sqrt{\log \alpha_1}))$ for Algorithm 1 in cDBGs. The question whether this can be improved, either by improving Dijkstra's algorithm (exploiting more properties of a cDBG) or by using a different approach, remains open.

Acknowledgements This work was funded by the ANR-12-BS02-0008 (Colib’read); the French project ANR MIRI BLAN08-1335497; and the European Research Council under the European Community’s Seventh Framework Programme (FP7 /2007-2013) / ERC grant agreement no. [247073]10.

References

1. KisSplice’s manual. <http://kissplice.prabi.fr/documentation>, 2013.
2. R. K. Ahuja, K. Mehlhorn, J. B. Orlin, and R. E. Tarjan. Faster algorithms for the Shortest Path Problem. *J. ACM*, 37:213–223, 1990.
3. E. Birmelé, P. Crescenzi, R. A. Ferreira, R. Grossi, V. Lacroix, A. Marino, N. Pisanti, G. A. T. Sacomoto, and M.-F. Sagot. Efficient bubble enumeration in directed graphs. In *SPIRE*, volume 7608 of *LNCS*, pages 118–129, 2012.
4. M. Chen, R. A. Chowdhury, V. Ramachandran, D. L. Roche, and L. Tong. Priority Queues and Dijkstra’s Algorithm. Technical Report TR-07-54, 2007.
5. R. Chikhi and G. Rizk. Space-efficient and exact de Bruijn graph representation based on a Bloom filter. In *WABI*, volume 7534 of *LNCS*, pages 236–248, 2012.
6. T. H. Cormen, C. Stein, R. L. Rivest, and C. E. Leiserson. *Introduction to Algorithms*. McGraw-Hill Higher Education, 2nd edition, 2001.
7. M. G. Grabherr, B. J. Haas, M. Yassour, J. Z. Levin, and D. A. Thompson *et al.* Full-length transcriptome assembly from RNA-seq data without a reference genome. *Nat. Biotechnol.*, 29:644–652, 2011.
8. Z. Iqbal, M. Caccamo, I. Turner, P. Flicek, and G. McVean. De novo assembly and genotyping of variants using colored de Bruijn graphs. *Nat. Genetics*, 2012.
9. C.-L. Li, S. T. McCormick, and D. Simchi-Levi. The complexity of finding two disjoint paths with min-max objective function. *Disc. Appl. Math.*, 1990.
10. A. Mortazavi, B. Williams, K. McCue, L. Schaeffer, and B. Wold. Mapping and quantifying mammalian transcriptomes by RNA-Seq. *Nat. Methods*, 5:621–628, 2008.
11. K. Pruitt, T. Tatusova, W. Klimke, and D. Maglott. NCBI reference sequences: current status, policy and new initiatives. *Nucleic Acids Research*, 37(Database-Issue):32–36, 2009.
12. G. Robertson, J. Schein, R. Chiu, and R. Corbett *et al.* De novo assembly and analysis of RNA-seq data. *Nat. Methods*, 7:909–912, 2010.
13. G. A. T. Sacomoto, J. Kielbassa, R. Chikhi, R. Uricaru, P. Antoniou, M.-F. Sagot, P. Peterlongo, and V. Lacroix. KISSPLICE: de-novo calling alternative splicing events from RNA-seq data. *BMC Bioinformatics*, 13:S5, 2012.
14. M. H. Schulz, D. R. Zerbino, M. Vingron, and E. Birney. Oases: robust de novo RNA-seq assembly across the dynamic range of expression levels. *Bioinformatics*, 28:1086–1092, 2012.
15. E. Wang, R. Sandberg, S. Luo, I. Khrebtkova, L. Zhang, C. Mayr, S. Kingsmore, G. P. Schroth, and C. Burge. Alternative isoform regulation in human tissue transcriptomes. *Nature*, 456(7221):470–476, Nov 2008.